Spin transfer in bilayer magnetic nanopillars at high fields as a function of free-layer thickness

W. Chen[1], M. J. Rooks[2], N. Ruiz[2], J. Z. Sun[2], A. D. Kent[1]
[1]*Department of Physics, New York University, New York, NY 10003, USA and*
[2]*IBM T. J. Watson Research Center, P.O. Box 218, Yorktown Heights, NY 10598, USA*
(Dated: August 21, 2006)

Spin transfer in asymmetric Co/Cu/Co bilayer magnetic nanopillars junctions has been studied at low temperature as a function of free-layer thickness. The phase diagram for current-induced magnetic excitations has been determined for magnetic fields up to 7.5 T applied perpendicular to the junction surface and free-layers thicknesses from 2 to 5 nm. The junction magnetoresistance is independent of thickness. The critical current for magnetic excitations decreases linearly with decreasing free-layer thickness, but extrapolates to a finite critical current in the limit of zero thickness. The limiting current is in quantitative agreement with that expected due to a spin-pumping contribution to the magnetization damping. It may also be indicative of a decrease in the spin-transfer torque efficiency in ultrathin magnetic layers.

PACS numbers:

Spin transfer in magnetic nanopillar has become a major focus of experimental research [1, 2, 3] since Slonczewski and Berger's seminal theoretical work in 1996 [4, 5]. A spin current has been demonstrated to switch the magnetization direction of a small magnet at a specific current density, as well as to induce microwave excitations. There are applications of this effect to magnetic random access memory (MRAM) and high-frequency electronics [1, 6, 7]. It is of importance to determine the factors that control the critical current for magnetization dynamics for both the physics and technology of spin transfer. For instance, it is of interest to reduce the critical current for MRAM applications, and to increase it in magnetic sensor designs.

In Slonczewski's theory, spin transfer is an interface effect: spin-angular momentum is transferred to the background magnetization when the spin current enters the ferromagnet –within the first few atomic layers [8]. For one polarity of the current, this generates a torque on the magnetization that is opposed by bulk damping. As a result, there is a threshold current to excite magnetization dynamics that is proportional to the volume of the magnet or, equivalently, the threshold current density is proportional to the thickness of the magnetic layer. There are alternative models in which the spin-transfer interaction occurs on a longer length scale, which predict a decrease in the efficiency of the torque in very thin magnetic layers [9, 10]. It is also now widely appreciated that the magnetization damping in thin layers can be dominated by interfaces, in an effect known as "spin pumping" [11]. For these reasons it is of importance to study spin transfer in samples in which the layer thicknesses are varied to gain insight into the factors that determine the strength and length scales of the spin-transfer interaction.

Albert *et al.* [12] studied current-induced magnetization switching as a function of free-layer thickness at room temperature. Here thermal fluctuations are important and the intrinsic (zero temperature) critical current was determined by extrapolating from pulsed current measurements. The switching was between in-plane magnetized states, parallel and antiparallel to the fixed-layer magnetization. In this case, the in-plane shape anisotropy plays an important role in setting the energy barrier to reversal. The switching current was found to depend linearly on the free-layer thickness and to be zero in the limit of zero free-layer thickness, consistent with Slonczewski's model.

In this paper, we present studies of spin-transfer at low temperature and high magnetic fields in asymmetric magnetic nanopillars in which the free magnetic-layer thickness has been systematically varied. The phase diagram for magnetic excitations has been determined in fields perpendicular to the film plane, under which the in-plane anisotropy is a minor effect, and at low temperature (4.2 K), where thermal fluctuations can be neglected. Similar to the results of Albert *et al.* [12], we find that the critical current density, defined to be the current density at which there is a step change in junction resistance, is a linear function of the layer thickness. However, it extrapolates to a finite zero thickness intercept. This suggests that damping related to spin pumping sets a lower limit for the critical current density in ultra-thin magnetic layers, or that spin transfer occurs over a finite-length scale in the ferromagnet.

In magnetic nanopillars that consist of thick and thin magnetic layers separated by a nonmagnetic layer, the thick (fixed) layer polarizes the current and dynamics is induced in the thin (free) layer. The magnetization of the free layer can be described by the Landau-Lifshitz-Gilbert (LLG) equation with an additional spin-transfer torque term [4, 5]. In a macrospin model, which assumes that the two layers are uniformly magnetized:

$$\frac{d\hat{m}}{dt} = -\gamma\hat{m}\times H_{\text{eff}} + \alpha\hat{m}\times\frac{d\hat{m}}{dt} + \frac{\gamma a_J}{1+\eta\hat{m}\cdot\hat{m_P}}\hat{m}\times(\hat{m}\times\hat{m_P}). \quad (1)$$

$\hat{m}$ and $\hat{m}_p$ are unit vectors in the direction of magnetization of the free and fixed magnetic layers, respectively. γ is the gyromagnetic ratio. The second term on the right

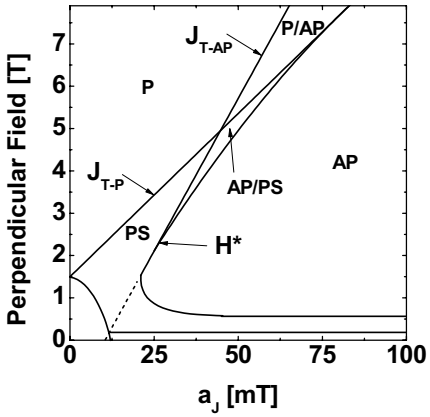

FIG. 1: Phase diagram of a nanopillar for $\eta = 0.3$, $\alpha = 0.01$, and $4\pi M_{\rm eff} = 1.5\ T$, with a small ($0.1\ T$) in-plane uniaxial anisotropy. The threshold current densities for instability of the P state, J_{T-P}, and for instability of the AP state, J_{T-AP}, are indicated.

is the damping term, where α is the Gilbert damping constant. The last term is due to spin-transfer. Here $a_J = \frac{\hbar J P_o}{2eM_s t}$, where J is the current density, P_o is the spin-polarization of the current, $M_{\rm s}$ is the magnetization density, and t is the free magnetic-layer thickness. The positive constant η characterizes the angular dependence of the torque and depends on the spin polarization [13]. The effective magnetic field $H_{\rm eff}$ is the vector sum of the applied field H, the in-plane anisotropy field $H_{\rm a}$, and the easy-plane anisotropy $-4\pi M_{\rm eff} m_z \hat{z}$, $H_{\rm eff} = H + H_a m_x \hat{x} - 4\pi M_{\rm eff} m_z \hat{z}$. In equilibrium, the magnetization is aligned with the effective magnetic field. The spin-transfer torque competes with damping, and at a threshold current density leads to excitation of the magnetization.

A phase diagram assuming a single-domain macrospin model can be calculated from Eq. 1, as shown in Fig. 1. For large fields perpendicular to the plane of the magnetic layers ($H > 4\pi M_{\rm s}$), the magnetizations of the fixed and free layer are aligned in the field direction. This is a particularly simple situation [2], as the in-plane shape anisotropy of the element plays only a minor role in the dynamics –the easy-plane anisotropy dominates, and the magnetic energy has axial symmetry. In this case, as J increases, the parallel (P) state becomes unstable at a threshold current:

$$J_{T-P} = \frac{2e\alpha}{\hbar P_o}(1+\eta) M_{\rm s} t (H - 4\pi M_{\rm eff}), \qquad (2)$$

leading to a precessional (PS) state. A further increase in the current results in the free layer switching into an antiparallel (AP) state. For a decreasing current, the AP becomes unstable and switches back to a PS or P state when:

$$J_{T-AP} = \frac{2e\alpha}{\hbar P_o}(1-\eta) M_{\rm s} t (H + 4\pi M_{\rm eff}). \qquad (3)$$

J_{T-P} and J_{T-AP} cross and become equal at the field $4\pi M_{\rm eff}/\eta$. However, hysteresis appears at a smaller field, H^*, corresponding to the lowest field at which the AP/PS region appears in the phase diagram. An interesting feature of the perpendicular field phase diagram is that the hysteresis is associated with the angular dependence of the spin-transfer torque [13]; the fact that the torque is larger in the AP state ($\eta > 0$). This is in contrast to conventional hysteresis in magnets, which is associated with dipolar interactions or magnetic anisotropy. Note that starting at large current and decreasing the current, the model predicts an abrupt and large change in the angle between the free and fixed layer at J_{T-AP}, which is detectable as a step change in junction resistance. This suggests that a measurement of the critical current on a decreasing current can be used to determine the AP threshold current (Eq. 3) as a function of magnetic field and sample structure. This is the approach we take in analyzing our experiments. While we will focus on the high-field behavior, we note for fields less than $4\pi M_{\rm eff}$ the layer magnetizations tilt into the film plane and the phase boundaries depend on the in-plane magnetic anisotropy.

Hundreds of pillar junctions with submicron lateral dimension were fabricated on a $1\times1\ cm^2$ silicon wafer using a nanostencil process [14]. Stencil holes with different but accurate lateral dimensions were opened up at the depth of $\sim 75\ nm$, and pillar junctions were deposited into those stencil holes through metal evaporation. Junctions have the layer structure $\|$ 3 nm Pt | 10 nm Cu | t Co | 10 nm Cu | 12 nm Co | 10 nm Cu | 3 nm Pt | 200 nm Cu $\|$. During the evaporation of the thin Co layer, we used a linear motion shutter to vary t from 1.8 to 5.3 nm across the wafer. Junctions with lateral dimensions 50×50, 50×100 and $70\times140\ nm^2$ were studied in detail.

All measurements reported here were made at 4.2 K with a 4-point geometry. Both dc resistance V/I and differential resistance dV/dI were measured for each junction. A $0.2\ mA$ modulation current at $802\ Hz$ was added to the dc bias. Junction resistances were found to scale inversely with lateral areas. Positive current is defined to be electron flow from the free (thin) Co layer to the fixed (thick) Co layer.

The magnetoresistance (MR) was measured with the magnetic field applied in the film plane. A typical MR hysteresis loop of a $50\times50\ nm^2$ junction with $t \simeq 2.8\ nm$ is shown in Fig. 2(a). The high resistance state corresponds to an AP state and for fields greater than $0.1\ T$ lead to a P state of lower resistance. The magnetoresistance, $MR = (R_{AP} - R_P)/R_P = \delta R/R_P$, is $(2.2\pm0.2)\%$, independent of the free layer thickness within the thickness range investigated (Fig. 1(c)). This shows that the MR is due mainly to spin-dependent scattering at Co/Cu interfaces. The MR area product, δRA, where A is the

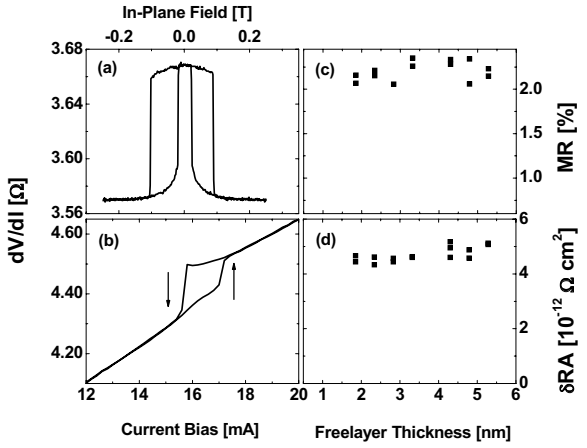

FIG. 2: (a) Zero dc current in-plane magnetoresistance hysteresis loop for a $50 \times 50\ nm^2$ junction with $t \simeq 2.8\ nm$. (b) Positive current sweep hysteresis loop of the same junction with perpendicular magnetic field set at 7 T. (c) MR of all junctions as the function of t. (d) Zero dc current in-plane δR times lateral area A for all junctions as the function of t.

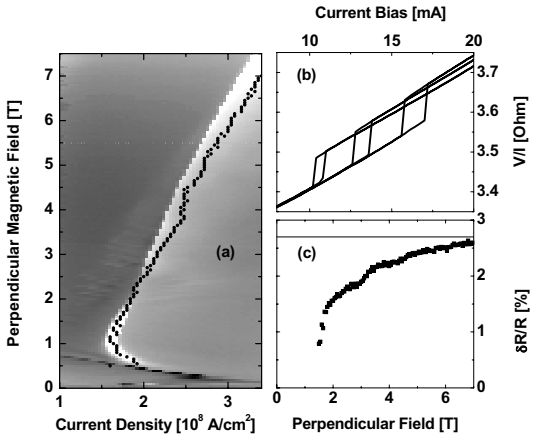

FIG. 3: (a) Contour plot of dV/dI minus a linear background as a function of both current density and magnetic field perpendicular to sample surface for decreasing current. The same junction as in Fig. 2 (a,b). "·" data points: The corresponding step in V/I for increasing current. (b) V/I *vs* current bias hysteresis loops with fields set at 3, 5 and 7 T. (c) $\delta R/R$ at the critical current as the function of field. Solid line: Zero dc current in-plane MR.

lateral area of the junction, is also independent of thickness, which indicates that δR is inversely proportional to the junction area, as expected.

Current-voltage measurements were conducted with a magnetic field applied perpendicular to the sample surface. Fig. 2(b) shows a current sweep hysteresis loop of the same junction as in Fig. 2(a) with a 7 T applied field. When the current is swept up to a sufficiently large value, 17.1 mA in this case, a step increase in resistance is observed (indicated with an upward arrow in Fig. 2(b)). We interpret this step as indicating the current at which the junction switches into an AP state, as reported in Ref. [2]. For decreasing current there is a step down in differential resistance at 15.7 mA, which, as discussed, we associate with the linear instability threshold given in Eq. 3, J_{T-AP}. The current hysteresis is about 1.4 mA at this field. The majority of junctions show hysteresis in current sweep measurements for fields larger than 3 T and steps in both dV/dI and V/I [15]. The sharp step in V/I has been used to determine the critical current for all junctions.

A contour plot of dV/dI as a function of current and perpendicular magnetic field shows the variation of the critical current with the applied perpendicular field. In order to emphasize the change of resistance on top of the background, which is associated with Joule heating, we have plotted dV/dI minus a linear background versus current density. Fig. 3(a) shows data for decreasing current on the same junction as in Fig 2(a), (b). The brighter the color in the contour plot, the larger the junction differential resistance. The boundary between the bright and dark region is an abrupt step in differential resistance. The corresponding position of the abrupt step for increasing current is illustrated with black dots in Fig. 3(a). We note that this boundary is not as straight as the current sweep down boundary. This is the case for all junctions, which we believe has its origin in the fact that magnetization precession and possibly spatially non-uniform spin-wave modes of the free layer, are excited at currents just below this switching boundary (see Fig. 1). Above the demagnetization field ($\sim 1.5\ T$), the threshold current increases with the applied magnetic field, consistent with Eq. 3. Fig. 3(b) shows the steps in V/I at 3, 5 and 7 T. The hysteresis decreases with decreasing field, and vanishes at H^*. H^* is nearly independent of thickness, and is $2.5 \pm 0.3\ T$ for most junctions [15]. The change in DC resistance $\delta R/R$ at the threshold current as a function of field is shown in Fig. 3(c). The solid line at 2.7 % is the in-plane MR. $\delta R/R$ increases with increasing field and asymptotically approaches the in-plane MR. In the macrospin model, more abrupt changes in magnetization state occur at higher magnetic field, due to the increasing importance of the angular dependence of the spin transfer torque, parameterized by η in our discussion. For example, for fields greater than $4\pi M_{\rm eff}/\eta$, the model predicts switching between AP and P states at J_{T-AP} and thus the full MR. Fig. 3(b) also shows that there is slight increase in the resistance at high current as the field increases.

About 20 junctions with different t and lateral dimensions were measured. The critical-current densities J_c as a function of magnetic field for all junctions were measured and analyzed, and 4 of the junctions, representing different free-layer thicknesses, are plotted in Fig. 4(a). From the figure, it is clear that the critical current increases with thickness at fixed magnetic field. The criti-

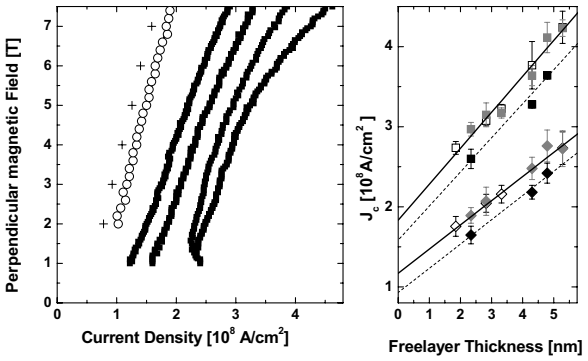

FIG. 4: (a) Solid points: critical-current density *vs* perpendicular magnetic field of 4 of the 50 nm series junctions with $t = 1.9,\ 2.8,\ 4.3,\ 5.3\ nm$ (from left to right). Open circles: critical current densities of all 50 nm series junctions extrapolated to zero t. Crosses: those of $70 \times 140\ nm^2$ junctions. (b) Critical current densities as a function of free layer thickness. Squares: 7 T. Diamonds: 3 T. Open, gray and black data points are the ones of 50×50, 50×100 and $70 \times 140\ nm^2$ junctions respectively. Solid lines: linear fits of critical current densities *vs* t of 50 nm series. Dashed lines: those of $70 \times 140\ nm^2$ junctions.

cal current density at a fixed field for all junctions is plotted in Fig. 4(b) as a function of a free-layer thickness, with different symbols (open, gray, and black) denoting the three studied junction sizes, as shown in the caption. The critical current density increases linearly with thickness, with a slope that increases with increasing field. This linear dependence is similar to the results of [12].

One interesting result from Fig. 4(b) is that the critical current density J_c also shows an observable dependence on lateral dimension. In our data, critical current densities of $70 \times 140\ nm^2$ junctions are generally lower than those of the 50×50 and $50 \times 100\ nm^2$ junctions (denoted the 50 nm series for ease of reference). As a result, 50 nm series (solid lines) and $70 \times 140\ nm^2$ junctions (dashed lines) were fit separately. In order to show the trend within the same series, 4 typical switching boundaries only from the 50 nm series were plotted in Fig. 4(a). From Fig. 4(b), the J_c shift of the $70 \times 140\ nm^2$ junctions from that of the 50 nm series is independent of the free-layer thickness, as the linear fits of the two different lateral series are parallel to each other.

We find that the intercepts of J_c *vs* t at different fields are not zero, as seen from the linear fits in Fig. 4(b). The intercepts, denoted by J_{c0}, of the 50 nm series are plotted as circles in Fig. 4(a), which is the "switching boundary in the limit of *zero free-layer thickness*." The corresponding boundary of the $70 \times 140\ nm^2$ junctions is plotted as the crosses in the same figure. J_{c0} is field dependent, which shows that dJ_{c0}/dH is nonzero. Because of the curvature of J_c *vs* H at high field for thicker free layers, dJ_c/dH becomes field dependent, and dJ_c/dH *vs* t turns out to be nonlinear. Therefore, the extrapolation of dJ_c/dH to zero thickness becomes ambiguous. Interestingly, J_c at a fixed field shows a linear dependence on thickness despite the curvature (Fig. 4). This linear dependence unambiguously gives a finite intercept of J_c at zero free-layer thickness. Note that although the curvature of the measured switching thresholds increases at high fields for thicker free layers, the slope of J_{c0} *vs* H is constant from 2 to 7 T.

J_{c0} is affected by the lateral dimension, since there is a shift between the boundaries of the two series. However, these two boundaries are parallel to each other, which shows that dJ_{c0}/dH is independent of the lateral dimension. $dJ_{c0}/dH = (1.5 \pm 0.3) \times 10^7\ A/cm^2T$ for both *zero free-layer thickness* boundaries, while Eq. 3 predicts $dJ_{c0}/dH = \frac{2e\alpha}{\hbar P_o}(1-\eta)M_s t|_{t=0} = 0$.

The lateral dimension of the pillars affects the critical currents, in that a constant shift of the critical-current densities between the 50 nm series and $70 \times 140\ nm^2$ was observed. Micromagnetic analysis of thin disks [16, 17] shows that the principle mode of the free layer is influenced by the lateral dimension and aspect ratio. As the result, the mode frequency depends on the lateral dimension. Since the critical current is proportional to the mode frequency, the change in the normal mode frequency is expected to shift the intercept of J_c *vs* H, while not changing dJ_{c0}/dH. Experimentally dJ_{c0}/dH is not found to depend on lateral dimension. Furthermore, in contrast to the prediction of Eq. 3, the threshold boundaries of most junctions do not extrapolate to $-4\pi M_{\rm eff}$ at zero current. Similarly, this may also be associated with the shift of the normal mode precessional frequency.

We note that Brataas *et al.* has recently computed the critical current for the excitation of non-uniform spin-wave modes [18]. The critical current density, considering the effect of the non-uniform modes, was found to depend linearly on magnetic-layer thickness –provided the excitation of such modes is opposed by bulk Gilbert damping.

The magnetic anisotropic field associated with the easy plane anisotropy is given as $4\pi M_{\rm eff}$. Based on an FMR study on extended Co films [19], $4\pi M_{\rm eff}$ is a function of Co thickness. In the thickness range studied here, $4\pi M_{\rm eff}$ changes as $1/t$, and it increases only by 0.2 T when Co thickness decreases from 5.3 to 1.9 nm. So anisotropy is also a minor effect, which cannot be the main contribution to the non-zero dJ_{c0}/dH.

There are two possible explanations for the observation of nonzero dJ_{c0}/dH. The first is associated with an interface contribution to the magnetization damping. Recently, Tserkovnyak *et al.* [11] employed a scattering theory approach to characterize this contribution to the damping for a thin ferromagnetic layer in contact with normal metals. They consider the spin current into adjacent normal layers (N) when there is magnetization dynamics. When such a spin current is dissipated by spin-flip scattering in the N layers, it generates additional

damping. We can estimate this additional contribution to the damping from the Tserkovnyak *et al.* theory, assuming that the Co layer is surrounded by perfect spin sinks, one of which is the fixed magnetic layer, and the other of which is a Pt layer, separated by 10 nm of Cu from the thin Co layer. The additional spin-pumping contribution to the damping is $\alpha' \simeq 1.7 \times 10^{-2}\ nm/t$, and is consistent with our recent FMR studies on similar structures [19]. As a result the net damping is $\alpha = \alpha_o + \alpha'$, where α_o is the bulk damping. With an interface contribution to the damping, the threshold current goes to a finite value in the zero thickness limit. Quantitatively, taking $\eta = 0.3$ and $P_o = 0.3$, we find $dJ_{c0}/dH = 1.4\times10^7\ A/cm^2T$, which is to be compared to our experimental result of $1.5\times10^7\ A/cm^2T$. This quantitative agreement suggests interfacial damping plays a significant role in determining the critical current density in spin-transfer devices.

An alternative explanation for our results is due to Zhang and Levy [9, 10]. In their model, the transverse component of spin decays on a length scale of λ_J in the ferromagnet, which they find is about 3 nm for Co. As a result, for layers of order and less than λ_J, the efficiency of the spin-transfer torque decreases –as the transverse component of angular momentum is not fully transferred to the thin magnetic layer. dJ_{T-AP}/dH decreases to a $t = 0$ limit of $\frac{2e\alpha_o}{\hbar P_o}\lambda_J(1-\eta)M_s = 1.0\times10^7\ A/cm^2T$, with $\alpha_o = 0.01$ [19]. This is also close to what we observe in experiment.

In summary, the phase diagrams for spin-transfer-induced magnetic excitations are experimentally determined in perpendicular magnetic field as a function of free-layer thickness. Based on the macrospin model (Fig. 1) and the observed hysteresis, we estimate the ratio of the torque in the AP state to that in the P state, due to its angular dependence, to be approximately 2 for a constant current. Further, we have found that the critical-current density for spin-transfer excitations is a linear function of free-layer thickness that extrapolates to a finite critical current at zero free-layer thickness. We have highlighted the role of the spin-pumping contribution to the damping, which can quantitatively explain our results. An implication of these results is that reducing the thickness of the magnetic layers permits a reduction of the critical-current density only to a lower limit set by interface effects.

We thank P. M. Levy for many useful discussions of this work. This research is supported by NSF-DMR-0405620 and by ONR N0014-02-1-0995.

[1] J. A. Katine, F. J. Albert, R. A. Buhrman, E. B. Myers, D. C. Ralph, Phys. Rev. Lett. **84**, 3149 (2000).
[2] B. Özyilmaz, A. D. Kent, J. Z. Sun, M. J. Rooks, R. H. Koch, Phys. Rev. Lett. **93**, 176604 (2003).
[3] S. Urazhdin, W. P. Pratt Jr., J. Bass, J. Magn. Magn. Mater. **282**, 264 (2004).
[4] J. C. Slonczewski, J. Magn. Magn. Mater. **159**, L1 (1996).
[5] L. Berger, Phys. Rev. B **54**, 9353 (1996).
[6] S. I. Kiselev, J. C. Sankey, I. N. Krivorotov, N. C. Emley, R. J. Schoelkopf, R. A. Buhrman, D. C. Ralph, Nature **425**, 380 (2003).
[7] W. H. Rippard, M. R. Pufall, S. Kaka, S. E. Russek, T. J. Silva, Phys. Rev. Lett. **92**, 027201 (2004).
[8] M. D. Stiles, A. Zangwill, Phys. Rev. B **66**, 014407 (2002).
[9] J. Zhang, P. M. Levy, Phys. Rev. B **70**, 184442 (2004).
[10] J. Zhang, P. M. Levy, Phys. Rev. B **71**, 184426 (2005).
[11] Y. Tserkovnyak, A. Brataas, G. E. W. Bauer, B. I. Halperin, Rev. Mod. Phys. **77**, 1375 (2005).
[12] F. J. Albert, N. C. Emley, E. B. Myers, D. C. Ralph, R. A. Buhrman, Phys. Rev. Lett. **89**, 226802 (2002).
[13] Z. Li, J. He, S. Zhang, Phys. Rev. B **72**, 212411 (2005).
[14] J. Z. Sun, D. J. Monsma, D. W. Abraham, M. J. Rooks, R. H. Koch, Appl. Phys. Lett. **81**, 2202 (2002).
[15] One exception is that hysteresis was not found on a $50\times50\ nm^2$ junction with a 5.3 nm free layer. This could be due to the strong coupling between the magnetic layers when free layer is sufficiently thick.
[16] R. D. McMichael, M. D. Stiles, J. Appl. Phys. **97**, 10J901 (2005).
[17] G. N. Kakazei, P. E. Wigen, K. Yu. Guslienko, V. Novosad, A. N. Slavin, V. O. Golub, N. A. Lesnik, Y. Otani, Appl. Phys. Lett. **85**, 443 (2004).
[18] A. Brataas, Y. Tserkovnyak, G. E. W. Bauer, Phys. Rev. B **73**, 014408 (2006).
[19] J.-M. L. Beaujour, W. Chen, A. D. Kent, J. Z. Sun, J. Appl. Phys. **99**, 08N503 (2006).